Periodic and turbulent behavior of solitary structures in distributed active media

H. Willebrand, T. Hünteler, F.-J. Niedernostheide, R. Dohmen, and H.-G. Purwins
Institute of Applied Physics, University of Münster, Germany
(Received 3 December 1991)

In a dc gas-discharge system we observe experimentally periodic and turbulent behavior of solitary structures, the latter having the form of filaments. It can be shown that turbulence develops due to four kinds of fundamental interactions between the solitary structures: creation, annihilation, elastic reflection, and clustering. It is believed that the experimental results are of general importance for pattern formation in distributive active media.

PACS number(s): 51.50.+v, 52.80.−s

I. INTRODUCTION

The spontaneous generation of inhomogeneous structures in dissipative active media can be found in biological [1,2], chemical [3–5], physical [6–9], and many other systems far from thermodynamic equilibrium. One of the most astonishing features of these patterns is that although they originate from different branches of science, there exist some fundamental structure elements which look quite the same. Notice, for example, the similarity of spiral wave patterns in the Belousov-Zhabotinskii reaction [10] and in dense cell layers of the slime mold [11]. Another example is the appearance of meanderlike structures in gas-discharge systems [12,13], hydrodynamic systems [14], and biological systems [15]. From these and other examples one may conclude that in many cases there exist fundamental building elements from which patterns in dissipative active systems can be constructed.

Elementary building elements in the form of filaments have been found e.g., in special lateral gas-discharge systems [12,13,16–21] but also in semiconductor materials [22–27], electrical networks [28,29], and various other dissipative active systems. In the present article we investigate the above-mentioned special gas-discharge device consisting of a semiconductor anode and a metallic cathode which are separated by a narrow discharge gap. In earlier experiments we found besides spatially inhomogeneous structures commonly known as current-density filaments [17,20] also spatially periodic patterns [18] which are discussed in the literature also under the name Turing structures. Spatiotemporal patterns in the form of splitting filaments [12,13], traveling-wave patterns [19], or spatiotemporal chaotic motion of current-density filaments [12,13] have also been observed. Many of these patterns could be found as solutions of a phenomenological reaction-diffusion model equation which has been investigated by means of analytical and numerical methods [8,13,16,18,21–24,30]. Also, swinging internal layer solutions have been found in a two-component reaction-diffusion system [31].

This contribution deals with current-density patterns in the form of standing filaments or filaments rocking between the boundaries of the discharge gap. Turbulence can be found if several filaments are generated. The interactions of the filaments can be of four different kinds: creation, annihilation, elastic reflection, and clustering. These interactions are believed to be of fundamental importance not only for our special gas-discharge device but also for other dissipative active systems. The rest of this article is organized as follows. In Sec. II we give a description of the experimental setup and the electrical and optical data recording system. In Sec. III the experimental results are discussed in detail. Finally, in Sec. IV we discuss the results and draw some conclusions.

II. EXPERIMENTAL SETUP

In Fig. 1 a schematic drawing of the experimental setup can be seen. The gas-discharge device is a two-electrode system. The cathode is made of copper and the anode consists of a high ohmic semiconductor material made of commercially available doped silicon with a specific resistivity on the order of some kΩ cm. In order to connect the semiconductor anode to the external circuit we have prepared an ohmic stripe contact at one side of the electrode by using a conventional diffusion technique in connection with a photolithographic process. The metallizing of the contact follows from vacuum deposition with a thin aluminum layer in a high vacuum system. The whole electrode arrangement is of rectangular shape with typical dimensions $l=30$ mm, $a=3$ mm, $b=10$ mm, and $d=0.3$ mm. We note that the value of d is very small in comparison to the other dimensions of

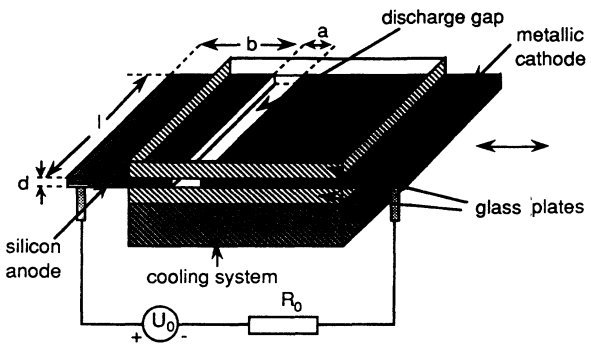

FIG. 1. Experimental setup of the gas-discharge device.

the discharge gap and therefore one may consider the system as being quasi one dimensional. To assure a one-dimensional discharge behavior in addition two glass plates cover the discharge gap from the bottom and from the top such that the discharge takes place only between the face plates of the electrodes. A water-cooling system guarantees approximately constant temperature during the operation of the device. This precaution is necessary because there is considerable heat production in high current regions. The described device is mounted in a vacuum receptacle which is provided with a glass window to ensure visual observation of the discharge pattern. For all experiments described in this article the vacuum receptacle is filled with argon. To drive the gas-discharge device we use a high-voltage power supply generating voltages U_0 up to 3500 V at a peak current I of 40 mA. The whole discharge system is connected to this voltage source via a load resistor which can be varied between some kΩ and 2 MΩ.

In the experimental investigations we are interested in the spatiotemporal behavior of current-density distributions appearing in the discharge gap. For the observation of the latter we use a streak-camera system combined with a high-speed digital oscilloscope. The complete measuring setup is shown schematically in Fig. 2. The most significant part of the measurement arrangement is the streak camera which operates as follows. The light emitted from the gap of the gas-discharge system is projected via a lens system onto a slit diaphragm placed at the entrance of the streak tube. The resulting slit image is focused on the surface of a photocathode. The photocathode converts the incident light into electrons. By applying a voltage of a few thousand volts between the photocathode and a mesh electrode placed very close to the front of the photocathode the electrons are accelerated in the direction of an electron deflection system. A ramp voltage generator provides a sawtooth pulse to the deflection plates just at the time when the incoming electron beam enters the deflection system. This results in a deflection of the electron beam along the vertical direction. After having passed the deflection field the electrons enter a microchannel plate, the function of which is to amplify the electron beam. The amplified electro-optical streak image is subsequently converted into a visible image on a phosphor screen. Due to the deflection of the electron beam from the top to the bottom of the phosphor screen the vertical axis represents the time axis, whereas the horizontal axis is the space coordinate. The final streak image contains the spatiotemporal information about the incident light and since the light intensity is proportional to the electrical current density within 5% we are able to measure the current-density distribution rather directly. The temporal resolution can be modified by changing the slope of the sawtooth voltage applied to the deflection plates. Finally, a silicon intensifier target camera picks up the streak image and the resulting video signal is fed to an image processing unit. For a more detailed description of the function of the streak-camera systems, see Refs. [32,33].

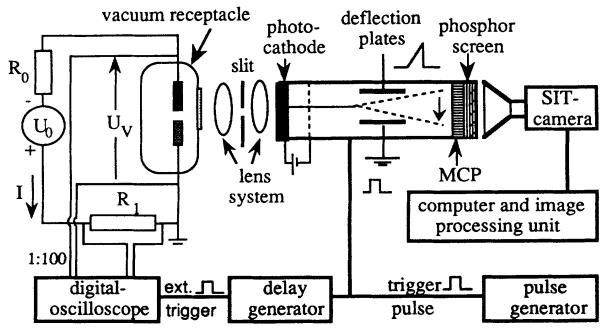

FIG. 2. Setup for measuring the spatiotemporal behavior of the current-density distribution in the discharge gap.

Besides the measurement of the spatiotemporal behavior by means of the streak-camera system we use a digital oscilloscope to measure the voltage U_V across the discharge device and the value of the total current I. The current is determined from the voltage drop across the resistor R_1 and the voltage across the discharge is measured by using a probe with a division ratio of 100:1. The pulse and the delay generator allow for the synchronization of the streak-camera record and the digital oscilloscope to make the measurement in the same time interval. This is possible because the streak unit has a fixed but well-known delay time t_d between the arrival of the trigger pulse and the firing of the camera. The delay generator, the output signal of which is applied to the external trigger input of the oscilloscope, serves to compensate this effect by generating a delayed output signal with the delay time t_d.

III. EXPERIMENTAL RESULTS

The experiments described in this section have been carried out in an argon atmosphere at gas pressures between 10 and 20 hPa using two different semiconductor electrodes with specific resistivities of 2600 and 900 Ω cm, respectively. In what follows we will call the former high- and the latter low-resistivity electrodes. In both cases the generation process of rocking filaments is similar for low values of the driving voltage U_0 or the average total current, but especially for large U_0 the system shows a different behavior. In the following we will first discuss some general features of rocking filaments in both systems and then point out the differences in the high- and low-resistivity cases. In this connection we point out that a system parameter that we can change easily is the external driving voltage U_0 (see Figs. 1 and 2). However, in gas-discharge physics the total current I or the averaged total current I_a are the most important quantities. Therefore, though in the strict sense the latter are not parameters in our setup, we have often chosen these quantities to describe the gas-discharge patterns, occasionally stressing that in reality the voltage U_0 is predetermined. In addition, the latter is always given in the figure captions.

A. Some general features

Under certain conditions an increase of the external applied voltage U_0 leads to the breakdown of the voltage

drop U_V at the device. The breakdown goes along with a large increase of the current I. Choosing appropriate outer circuit parameters one observes the appearance of a lightening region between the electrodes. Looking at the discharge gap with the naked eye one can see a homogeneously glowing discharge region filling a part of the discharge gap. In the direction of the current flow a stratification of the discharge pattern can be observed. A further increase of the voltage U_0 leads to a further increase of the current I and to a broadening of the lightening area until finally the whole gap is homogeneously lightening. Up to this point one would expect to investigate a homogeneous stationary discharge pattern, but if we measure with the oscilloscope the voltage drop U_V across the discharge device and the total current I flowing through the system we notice that the behavior is much more complicated. Figure 3 shows the plot of a typical time series taken just above the breakdown voltage. In the upper part of Fig. 3 we see the corresponding current signal I and in the lower part the voltage signal U_V. Therefore exceeding the breakdown voltage does neither lead to a stationary voltage drop U_V nor to a constant current flow I.

From Fig. 3 it follows that the current oscillations exhibit a spikelike behavior while the corresponding voltage oscillations are comparatively smooth: The current varies between 0.22 and 0.62 mA, whereas the voltage shows a modulation of about 20 V at an average value of approximately 370 V. We also note that the current signal has an additional fast modulation. By performing streak-camera measurements we will now show that it is possible to find a correlation between the temporal oscillations in the current and the voltage on the one hand, and spatiotemporal oscillations of the light (current) density distribution in the discharge gap on the other hand.

In Fig. 4 we represent a three-dimensional plot of a streak image taken from the positive column of the discharge gap. This spatiotemporal signal is measured simultaneously with the oscillations shown in Fig. 3. The total recording time of the streak image has been about 700 μs and the imaging system has been positioned in such a way that the image of the discharge gap of length l (see Fig. 1) covers precisely the input slit of the camera. The third axis is the measured light density.

From Fig. 4 it becomes obvious that the current and voltage oscillations are accompanied by the periodic motion of a single well-defined region of high light density which we consider as an elementary building element of the dynamic pattern that we observe. In what follows we call this object a "filament." Therefore the observed pattern can be described in terms of a filament rocking between the boundaries of the discharge gap. The rocking filaments appear instantaneously at the boundary of the gap when the breakdown voltage is exceeded. When the filament reaches the boundary it is reflected and moves in the opposite direction while the shape of the filament stays the same and the velocity remains constant. The process is repeated when the filament reaches the opposite boundary. Therefore we conclude that we observe a periodic spatiotemporal oscillation of one filament reminding us of a billiard ball elastically reflected at the edges of the table. Consequently, the first kind of interaction that we observe is an elastic reflection which in this case takes place at the boundary. If we look very close to Fig. 4 we realize that for a very short time just at the beginning of the generation process two filaments appear; just one of them at each boundary. However, after about 70 μs one filament extinguishes while the other one moves with constant velocity towards the boundary of the gap. This is the second kind of interaction that we observe and we call it annihilation, in this case due to a collision between two filaments. Because the shape and velocity of the filament remain unchanged after the interaction the filament has a "solitary" character.

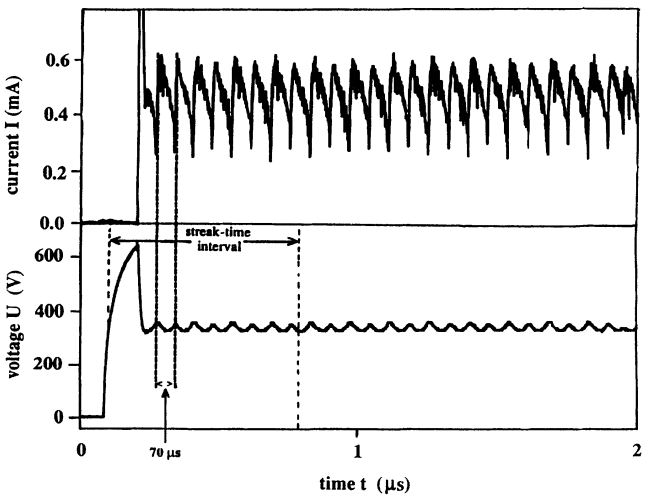

FIG. 3. Measured current I (upper part) and voltage $U=U_V$ (lower part) just above the breakdown of the voltage drop across the discharge device. The explanation of the marked time intervals is given in the text. The parameters are $l=28$ mm, $b=8$ mm, $d=0.25$ mm, $\rho=2.6$ kΩ cm, $p=18$ hPa, $a=3.4$ mm, $R_0=1$ MΩ, and $U_0=990$ V.

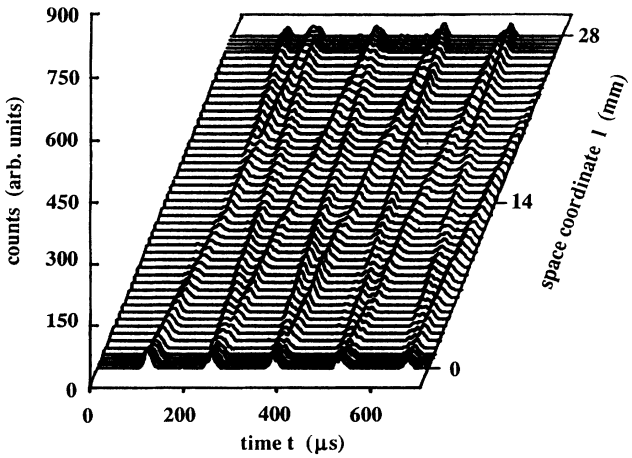

FIG. 4. Three-dimensional streak-camera image showing the spatiotemporal behavior of a rocking filament just above the breakdown of the voltage drop across the discharge device. The streak camera image has been taken simultaneously with the measurement shown in Fig. 3 (see the streak-time interval marked in Fig. 3).

If we look more closely at the correlation between the temporal and the spatiotemporal behavior we notice that the time interval between the spikelike current oscillations in Fig. 3 is about 70 μs. Figure 4 confirms that this is the time the filament needs to move from one boundary of the discharge gap to the opposite one. In addition, we notice that the current I always reaches a minimum and the voltage U_V a maximum value when the rocking filament is reflected at the edge of the gap. In other words, the resistivity of the gas-discharge device reaches its maximum value when the filament is situated at the boundary. When the filament reaches the boundary the current changes very rapidly, whereas the change of the voltage is more slowly.

By increasing the temporal resolution of the streak-camera system it has been possible to find the reason for the additional modulation of the total current in Fig. 3. This is demonstrated in Fig. 5, where we have plotted the current I and voltage U_V on the left-hand side and the corresponding streak-camera image on the right-hand side using an increased time resolution.

From Fig. 5 it becomes obvious that the modulation of the time signals is not due to system noise produced by internal fluctuations which may appear in the gas-discharge system, but is due to a current modulation caused by a stratification process superimposed by the rocking of the filament. While the filament moves from one boundary to the opposite one the strata appear and vanish nearly 25 times. Experimental investigations on the stratification process between two metal stripe electrodes carried out in the gas discharge similar to that shown in Fig. 1 can be found in Ref. [34]. In what follows we will disregard the generation of strata and concentrate our interest on the rocking of filaments. To consider these effects separately is justified because the rocking of filaments and the generation of strata take place on different time scales and so far we did not find any hint for a coupling of these phenomena.

By increasing the voltage U_0 the average value I_a of the total current I increases too. At the same time not only the amplitudes of the current and voltage oscillations but also the velocity of the rocking filament are almost constant. However, the latter can be changed by varying the gas pressure. Figure 6 shows the measured velocity of a rocking filament as a function of the average value I_a of (a) the total current I and (b) the pressure p for a typical set of system parameters.

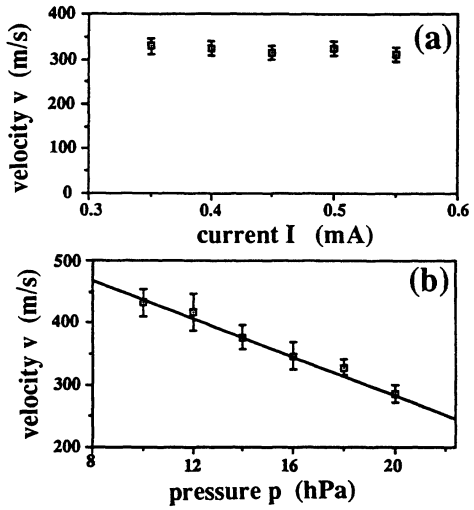

FIG. 6. Velocity v of a rocking filament as a function of the average value I_a of (a) the total current I and (b) the pressure. The parameters are as follows. (a) $l=28$ mm, $b=10$ mm, $d=0.28$ mm, $\rho=0.9$ kΩ cm, $p=19$ hPa, $a=4.8$ mm, $R_0=1$ MΩ. U_0 was changed from 690 V at $I_a=0.35$ mA to 890 V at $I_a=0.55$ mA. (b) $l=28$ mm, $b=10$ mm, $d=0.28$ mm, $\rho=0.9$kΩ cm, $a=4.7$ mm, $R_0=1$ MΩ. This measurement has been taken at an average total current of $I_a=0.4$ mA. To maintain constant current U_0 was changed from 734 V at 20 hPa to 751 V at 10 hPa.

The measurements represented in Fig. 6(a) have been taken at a gas pressure of $p=19$ hPa. Between $I_a=0.35$ and 0.55 mA a filament appears, moving with a constant velocity of about 320 m/s between the boundaries of the discharge gap. The retention of a constant velocity of the rocking filament has been found in the whole pressure range between 10 and 20 hPa, whereby the current interval where the velocity stays constant depends on the pres-

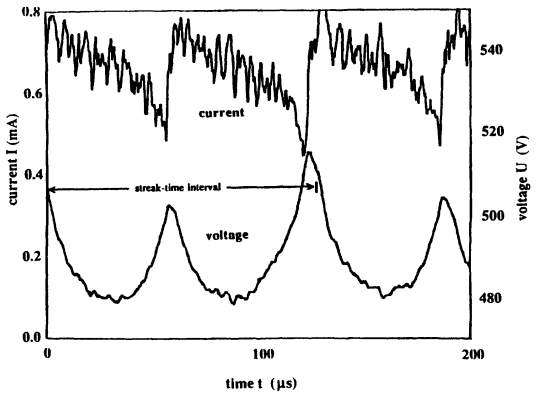

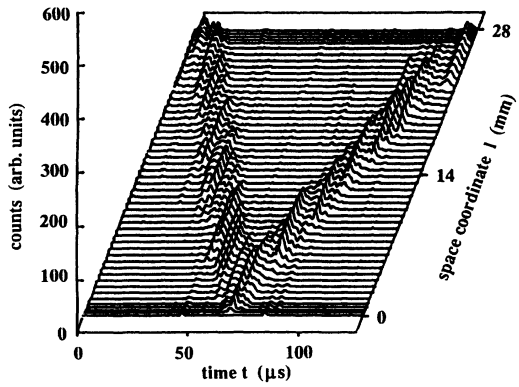

FIG. 5. Current I and voltage U_V (left-hand side) and plot of the simultaneously measured streak-camera image (right-hand side) recorded with relatively higher time resolution. The streak-time interval is marked in the diagram on the left-hand side. The parameters are $l=28$ mm, $b=8$ mm, $d=0.25$ mm, $\rho=2.6$ kΩ cm, $p=18$ hPa, $a=3.5$ mm, $R_0=1$ MΩ, and $U_0=1310$ V.

sure. Furthermore, the velocity of the rocking filament is not the same in the whole pressure interval between 10 and 20 hPa. In Fig 6(b) the dependence of the velocity v as a function of the pressure is represented. Within the limit of the uncertainty in the determination of the velocity from the streak image, there is a linear decrease of the velocity with increasing gas pressure.

The experimental results may raise the question of what happens outside the current and pressure intervals shown in Figs. 6(a) and 6(b). Concerning the pressure interval, we remark that up to now the rocking of filaments has only been observed at a pressure between 10 and 20 hPa. Especially, above 20 hPa a scenario resulting in the generation of multiple stationary filamentary structures has been observed [12,13,17]. Outside the current interval of constant rocking velocity the behavior of the system is quite different from the situation described above. For a rather small value of the total current the breakdown of the device voltage U_V leads to the generation of a filament at its boundary which moves instantaneously into the direction of the center of the gap. After having moved a short distance the filament extinguishes and the process is repeated. The distance the filament has traveled is influenced by the value of the current and it increases with increasing current, until finally, the filament reaches the opposite boundary. The rocking of the filament results from a further increase of the current. From the aforementioned we see that the filament can undergo also an interaction in the form of an annihilation but here in the form of a simple disappearance retaining the solitary character until it vanishes.

B. The high-resistivity case

So far the influence of the specific resistivity of the semiconductor electrode has not been discussed. However, for relatively large values of the total current it is possible to distinguish between a high- and a low-resistivity case. In this subsection we are going to discuss the high-resistivity case.

The series of photographs shown in Fig. 7 have been

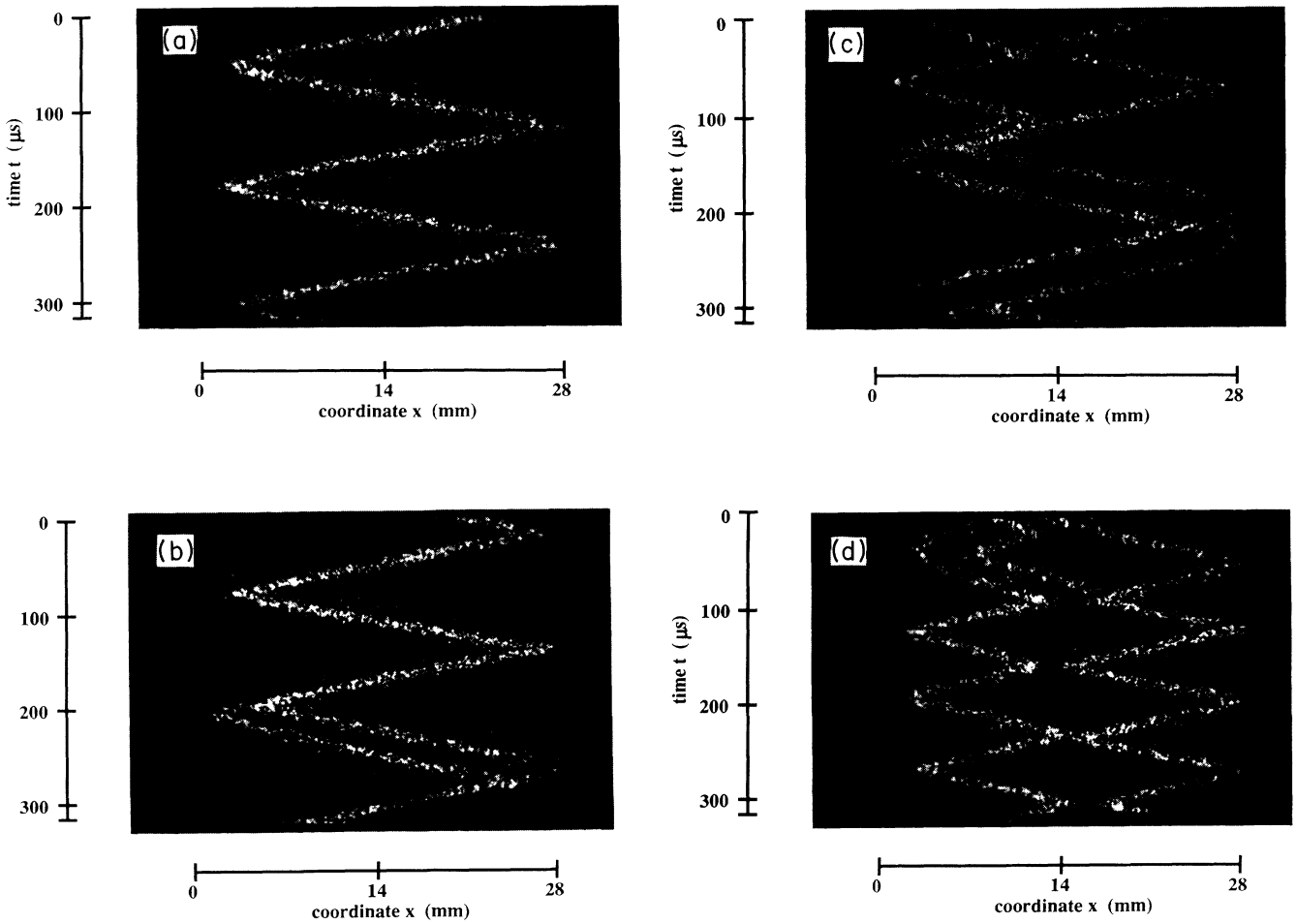

FIG. 7. Streak-camera photographs of rocking filament scenarios for the case of a high-resistivity electrode and for increasing averaged total current I_a. Due to the increase of the number of solitary filaments and due to their interactions turbulence appears. The parameters are $l=28$ mm, $b=8$ mm, $d=0.25$ mm, $\rho=2.6$ kΩ cm, $p=20$ hPa, $a=3.25$ mm, and $R_0=250$ kΩ. (a) $U_0=500$ V, $I_a=0.59$ mA; (b) $U_0=518$ V, $I_a=0.65$ mA; (c) $U_0=573$ V, $I_a=0.89$ mA; (d) $U_0=585$ V, $I_a=0.94$ mA; (e) $U_0=670$ V, $I_a=1.23$ mA; (f) $U_0=723$ V, $I_a=1.43$ mA; (g) $U_0=766$ V, $I_a=1.60$ mA; (h) $U_0=847$ V, $I_a=1.88$ mA.

taken with the streak-camera system using a semiconductor electrode of 2600 Ω cm. The vertical axis displays the time, the horizontal axis the space coordinate. The projection of the discharge gap onto the input slit of the streak unit (see Fig. 2) has been chosen in such a way that the spatiotemporal behavior of the light (current) density distribution of the whole discharge gap could be recorded. The exact gap position for the complete series of photographs is marked in Fig. 7(a): one boundary is located at $l=0$ mm and the other at $1=28$ mm. We note that the photographs shown here exhibit some distortion due to the curvature of the TV monitor from which the pictures were taken.

Figure 7(a) has been taken at a value of the averaged total current I_a where the filament is moving between the boundaries of the gap. The intensity modulation of the filament trace is due to moving striations, the appearance and behavior of which have been mentioned above. It becomes obvious that the filament is reflected within a time interval of a few microseconds at the boundaries. Especially, by using a higher temporal resolution of the streak camera it can be demonstrated that the filament does not extinguish at the boundary. Figure 7(b) has been taken after increasing I_a. This streak image shows the generation of a second filament by a splitting of the first one. Therefore we observe besides reflection and annihilation a third kind of interaction which is a creation of a filament due to splitting. This second filament does also rock for a short time interval but then disappears by a collision with the first one. This kind of interaction has been observed already in Fig. 4 and has been discussed above. Again, the solitary behavior of the filaments as fundamental building elements is demonstrated by the fact that the shape of the filaments is retained after interaction. For higher values of the total current these features become even more obvious as can be seen from Figs. 7(c) and 7(d).

In Fig. 7(c) two rocking filaments moving with nearly the same velocity are visible. Both of them are reflected when reaching the boundary of the discharge gap, but because the direction of motion can be opposite a collision between the two filaments is inevitable. Now different possible solutions of this "collision problem" can be observed which correspond to different kinds of interactions. One realization is the change of the direction of both filaments. This kind of interaction is a reflection, but this time an elastic repulsion of two filaments. Such a process can be seen in the upper part of Fig. 7(c). The second possibility is the change of direction of only one of

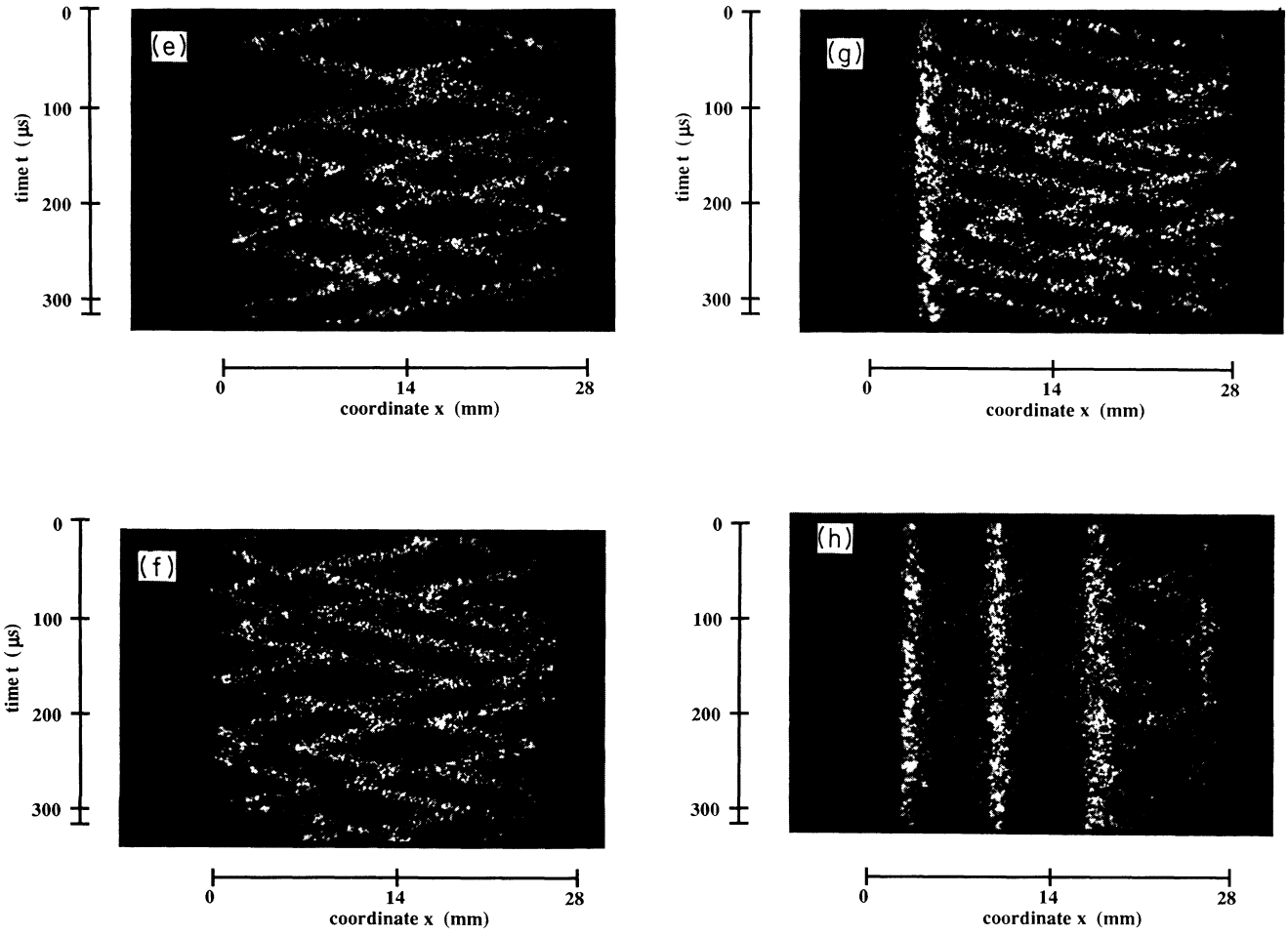

FIG. 7. (*Continued*).

the filaments, which means that one filament forces the other one to reverse the moving direction. This case can also be found in Fig. 7(c) after a recording time of 100 μs. We want to call this interaction "clustering" because one has the impression that one filament forces the other along its way. Such a situation can be seen also in Fig. 7(b). From other experiments we know that the probability of appearance of the first or the second process is mainly determined by the spatial position of the collision point. If two filaments strike each other near to the middle of the gap both of them change the direction of propagation; otherwise, the filament nearest to a boundary is forced by the second filament to change its direction of motion.

Figure 7(d), which results from Fig. 7(c) by increasing the current I_a further, gives the impression that the filaments try to arrange themselves in the gap in such a way that each of them moves in different but equally large areas and the interaction is mostly dominated by elastic reflection of two filaments. In addition, in the upper part of Fig. 7(d) a third rocking filament becomes visible during a short time interval. This filament disappears when it hits the rocking filament at the right-hand side of the gap and disappears due to annihilation interaction.

Figures 7(e) and 7(f) result from a further increase of the averaged total current I_a. Figure 7(e) has been taken at the transition regime between two and three rocking filaments. During a certain time interval there exist only two filaments but then, as a result of a creation interaction in the form of a division process, a third filament appears. On a longer time scale we will always find a competition between these two states. If there exist three filaments each of them also tries to claim equal areas in space. On the one hand, one may conclude that there is a certain tendency of the system to arrange a symmetric distribution in space, but on the other hand the disturbance of the structure due to collision and annihilation processes can be observed very often. This behavior can

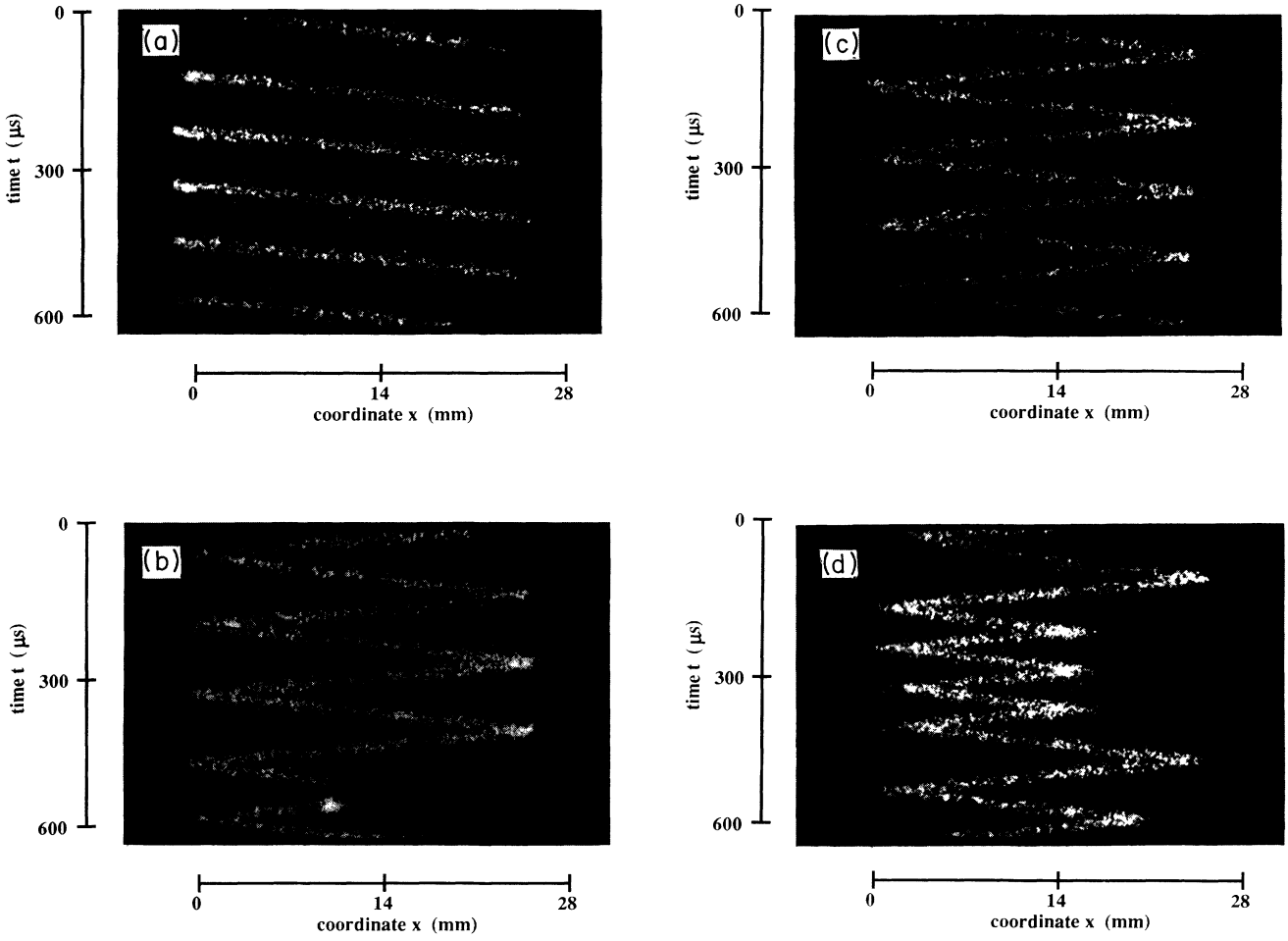

FIG. 8. Streak-camera photographs of the generation of rocking filaments for the low-resistivity semiconductor electrode system for increasing voltage U_0 corresponding to increasing average total current I_a. Due to the interaction of the filaments a turbulent behavior in the form of spatiotemporal intermittency appears. The parameters are $l=28$ mm, $b=10$ mm, $d=0.28$ mm, $\rho=0.9$ kΩ cm, $p=14$ hPa, $a=4.8$ mm, and $R_0=1$ MΩ. (a) $U_0=800$ V, $I_a=0.4$ mA; (b) $U_0=880$ V, $I_a=0.5$ mA; (c) $U_0=950$ V, $I_a=0.6$ mA; (d) $U_0=1090$ V, $I_a=0.74$ mA; (e) $U_0=1125$ V, $I_a=0.78$ mA; (f) $U_0=1340$ V, $I_a=1.0$ mA; (g) $U_0=1830$ V, $I_a=1.5$ mA; (h) $U_0=2010$ V, $I_a=1.7$ mA.

also be found in Fig. 7(f), where during the short time interval between 60 and 100 μs also four filaments appear. Therefore, this kind of spatiotemporal disorder can be called turbulent or more precisely spatiotemporal intermittence. It is interesting enough that the observed turbulence is based again on fundamental solitary building elements which have the shape of solitary filaments.

At high values of the total current besides rocking solitary filaments also stationary filaments do appear. In Fig. 7(g) the first evidence for the generation of a stationary filament is observed on the left-hand boundary of the discharge gap. In the remaining area the turbulent rocking continues and therefore we observe the interesting phenomenon of a simultaneous existence of stationary structures and turbulence. Figures 7(g) and 7(h) have been taken at values of the total current where one [Fig. 7(g)] and three [Fig. 7(h)] stationary filaments exist.

From many experimental investigations on the gas-discharge system described in this article we know that the positions in space where stationary filaments appear are not connected with spatial inhomogeneities. Before carrying out the experiments we carefully polish the surfaces of the electrodes and especially check the semiconductor electrode for spatial inhomogeneities of the specific resistivity. By applying a magnetic field or by irradiating the discharge gap with UV light it is also possible to displace the filaments in space. This behavior demonstrates that if there were inhomogeneities effecting the filaments, their influence must be very weak. Also, as can be seen from experiment the stationary pattern of Fig. 7(b), e.g., can appear but must not appear at other areas in space. In addition, it can be seen that there is no indication that the filaments moving with a constant velocity between the boundaries of discharge gap are affected by inhomogeneities. Therefore we believe that the structures observed in the present work are due to real self-organization of the system.

C. The low-resistivity case

In Fig. 8 a series of streak-camera photographs for a semiconductor electrode with low specific resistivity is shown. Note that the temporal resolution is not the same for all pictures. In Fig. 8(a) a filament appears at the left-hand boundary of the gap and moves with constant velocity to the opposite boundary where it disappears. This process is repeated periodically in space and time. For higher values of the driving voltage U_0 and therefore

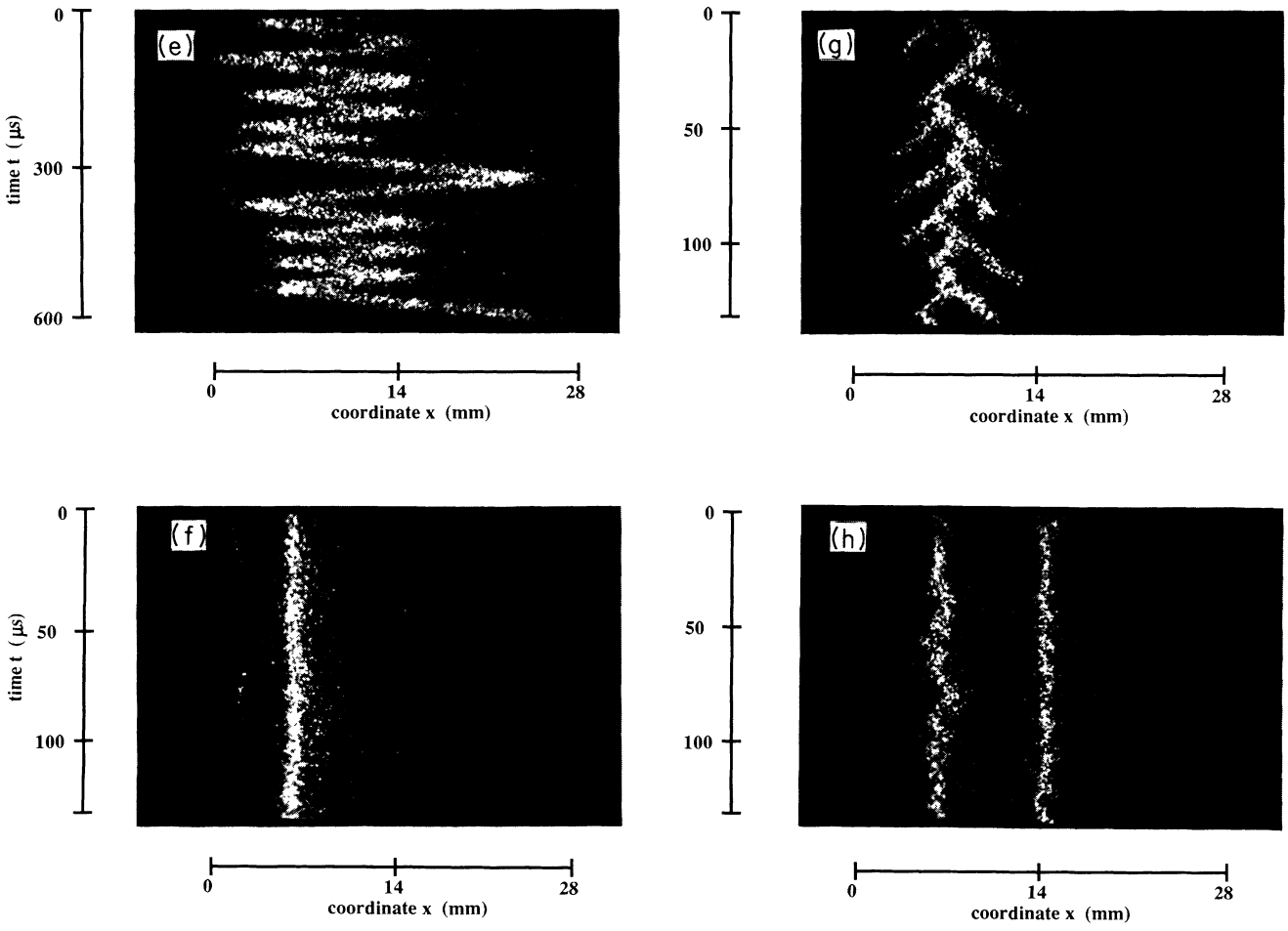

FIG. 8. (*Continued*).

for higher average total current the filament starts rocking between the boundaries. However, it may happen that the filament disappears for a short time interval and reappears to continue rocking [Fig. 8(b)]. A further increase of the current leads to a behavior which is very similar to that shown in Fig. 7(a).

So far there is no qualitative difference in the system behavior for the high- and the low-resistivity cases. The first significant difference becomes obvious in Fig. 8(d), where U_0 and I_a have been increased further. Contrary to the behavior described above, there is no generation of a second filament, but instead the rocking amplitude of the filament changes. The large-amplitude oscillations between the boundaries change to small-amplitude oscillations and vice versa. The time interval of small-amplitude oscillations increases by increasing the current, whereby the interval of large-amplitude oscillations decreases. This is demonstrated in Fig. 8(e). This behavior reminds us of temporal intermittency. Therefore we may call this kind of pattern spatiotemporal intermittence. At even higher values of the current the amplitude of oscillation decreases and finally as shown in Fig. 8(f) the filament becomes stationary. The generation of further filaments results from a splitting process which has already been observed in another parameter region [12]. In Fig. 8(g) a typical transition pattern from the one-filament state of Fig. 8(f) to a two-filament state is shown. The resulting pattern, consisting of two spatially separated filaments, is represented in Fig. 8(h).

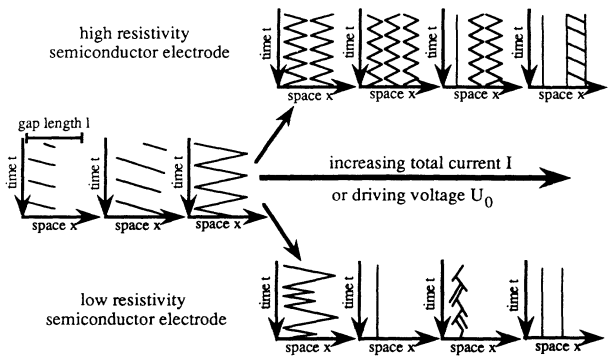

FIG. 9. Schematic representation of different kinds of rocking filaments for increasing total current I. The upper part shows the behavior for high resistivity, the lower part for low-resistivity semiconductor electrodes. For a rather small value of the total current I both systems are acting in the same way.

IV. SUMMARY AND CONCLUSIONS

Figure 9 gives a summary of the experimental findings of this article by schematically representing the spatiotemporal behavior of the gas-discharge system for increasing values of driving voltage U_0 or increasing total current I. The gap length l and its position are shown in the figure on the left-hand side. While the use of the high-resistivity semiconductor electrode leads to an increase of the number of rocking filaments by increasing the current, the use of the low-resistivity electrode does not lead to a change of their number. In the latter case the increase of the total current only affects the spatial amplitude of the rocking filament.

In all experiments discussed in this article the current-density distribution in the discharge gap appears in the form of elementary solitary building elements which we call filaments. The filaments can be characterized by some fundamental features.

(a) The width and the current density of the filaments are almost the same for a certain parameter set.

(b) The shape of a filament does not change when changing the system parameters.

(c) In a certain range of parameters rocking filaments do exist.

(d) Rocking filaments move with constant velocity between the boundaries of the discharge gap without changing the shape.

(e) The velocity of a rocking filament decreases with increasing gas pressure.

(f) Rocking filaments can undergo transitions to standing filaments and other structures as there are, e.g., pigtail structures [see Fig. 8(g)].

(g) Filaments can interact in four different ways: creation, annihilation, reflection, and clustering.

(h) The shape of the filaments is the same before and after an interaction.

(i) Due to the interaction of filaments complicated spatiotemporal structures may evolve and, e.g., turbulence can appear.

(j) Rocking filaments can coexist with stationary structures.

Comparing the present results with earlier investigations of similar gas-discharge systems [12,13,16–21], we recognize that all observed current density distributions can be interpreted in terms of filaments having the above properties. Patterns consisting of filaments have been observed also in many physical chemical, biological, and other systems [1–4,9,22–29,35,36]. We therefore conclude that the system investigated in the present article is a paradigm for a large class of systems, and consequently the results of this and related articles should be of general importance for understanding the mechanism of pattern formation in dissipative active media.

From gas-discharge physics one knows that the underlying microscopic mechanism leading to patterns as they are reported in this article are very complex, and therefore the theoretical description on a microscopic level may be very complicated. However, by using a simple two-component reaction-diffusion model it has been possible to describe qualitatively many features of systems of the kind that are investigated in the present article [8,13,18,21,22,24,30,31,36]. The corresponding model equations turn out to be of a very general type supporting again the importance of the results of this and related work.

ACKNOWLEDGMENT

The authors gratefully acknowledge the Stiftung Volkswagenwerk for the support of this work.

[1] P. C. Fife, in *Mathematical Aspects of Reacting and Diffusing Systems,* edited by S. Levin, Lecture Notes in Biomathematics Vol. 28 (Springer-Verlag, Berlin, 1979).
[2] J. D. Murray, *Mathematical Biology* (Springer-Verlag, Berlin, 1989).
[3] A. N. Zaikin and A. M. Zhabotinskii, Nature (London) **225**, 535 (1970).
[4] For general review, see R. J. Field and M. Burger, *Oscillations and Travelling Waves in Chemical Systems* (Wiley, New York, 1985).
[5] L. Lobban and D. Luss, J. Phys. Chem. **93**, 6530 (1989).
[6] H. Bénard, Rev. Gen. Sci. Pures Appl. **11**, 1261 (1900).
[7] G. Ertl, Phys. Bl. **46**, 339 (1990).
[8] H.-G. Purwins, Ch. Radehaus, T. Dirksmeyer, R. Dohmen, R. Schmeling, and H. Willebrand, Phys. Lett. A **136**, 480 (1989).
[9] B. S. Kerner and V. V. Osipov, Usp. Fiz. Nauk **157**, 201 (1989) [Sov. Phys. Usp. **32**, 101 (1989)].
[10] A. T. Winfree, Science **175**, 634 (1972).
[11] G. Gerrisch, Naturwissenschaften **58**, 430 (1971).
[12] H. Willebrand, F.-J. Niedernostheide, E. Ammelt, R. Dohmen, and H.-G. Purwins, Phys. Lett. A **153**, 437 (1991).
[13] H. Willebrand, F.-J. Niedernostheide, R. Dohmen, and H.-G. Purwins, in *Oscillations and Morphogenesis,* edited by L. Rensing (Marcel Dekker, New York, in press).
[14] C. W. Mayer, G. Ahlers, and D. S. Cannell, Phys. Rev. Lett. **59**, 1577 (1987).
[15] J.-B. Boon and A. Noullez, in *On Growth and Form,* edited by H. E. Stanley and N. Ostrowsky (NATO ASI Series E No. 100 (Academic, New York, 1986).
[16] C. Radehaus, R. Dohmen, H. Willebrand, and F.-J. Niedernostheide, Phys. Rev. **42**, 7426 (1990).
[17] H. Willebrand, C. Radehaus, F.-J. Niedernostheide, R. Dohmen, and H.-G. Purwins, Phys. Lett. A **149**, 131 (1990).
[18] C. Radehaus, H. Willebrand, R. Dohmen, F.-J. Niedernostheide, G. Bengel, and H.-G. Purwins, Phys. Rev. A **45**, 2546 (1992).
[19] H. Willebrand, K. Matthiessen, F.-J. Niedernostheide, R. Dohmen, and H.-G. Purwins, Contr. Plasma Phys. (to be published).
[20] Ch. Radehaus, T. Dirksmeyer, H. Willebrand, and H.-G. Purwins, Phys. Lett. A **125**, 92 (1987).
[21] H.-G. Purwins, Ch. Radehaus, and J. Berkemeier, Z. Naturforsch. **43a**, 17 (1988).
[22] Ch. Radehaus, K. Kandell, H. Baumann, D. Jäger, and H.-G. Purwins, Z. Phys. B **65**, 515 (1987).
[23] F.-J. Niedernostheide, B. S. Kerner, and H.-G. Purwins (unpublished).
[24] F.-J. Niedernostheide, R. Dohmen, H. Willebrand, H.-J. Schulze, and H.-G. Purwins, in *Nonlinearity with Disorder,* International Workshop, Taschkent, U.S.S.R., 1990, edited by A. Bishop, Springer Proceedings in Physics (Springer, Berlin, 1992).
[25] B. S. Kerner and V. F. Sinkevich, Pis'ma Zh. Eksp. Teor. Fiz. **36**, 359 (1982) [JETP Lett. **36**, 436 (1982)].
[26] H. Baumann, R. Symanczyk, C. Radehaus, H.-G. Purwins, and D. Jäger, Phys. Lett A **123**, 421 (1987).
[27] K. M. Mayer, J. Parisi, and R. P. Huebener, Z. Phys. B **71**, 171 (1988).
[28] J. Berkemeier, T. Dirksmeyer, G. Klempt, and H.-G. Purwins, Z. Phys. B **65**, 255 (1986).
[29] T. Dirksmeyer, R. Schmeling, J. Berkemeier, and H.-G. Purwins, in *Patterns, Defects and Materials Instabilities,* edited by D. Walgraef and N. M. Ghoniem, NATO ASI Series E, No. 183 (Academic, New York, 1989).
[30] R. Dohmen, Ph. D. thesis, University of Münster, 1991 (unpublished).
[31] Y. Nishiura and M. Mimura, SIAM J. Appl. Math. **49**, 481 (1989).
[32] Y. Tsuchiya, IEEE J. Quantum Electron. **QE-20**, 1516 (1984).
[33] D. J. Bradley, S. F. Bryant, J. R. Taylor, and W. Sibbett, Rev. Sci. Instrum. **49**, 215 (1978).
[34] E. Ammelt, H. Willebrand, and H.-G. Purwins, Contr. Plasma Phys. (to be published).
[35] H.-G. Purwins and Ch. Radehaus, *Pattern Formation on Analogue Parallel Networks,* Springer Series on Synergetics Vol. 42 (Springer-Verlag, Berlin, 1988).
[36] R. Dohmen, F.-J. Niedernostheide, N. Reese, H. Willebrand, and H.-G. Purwins (unpublished).

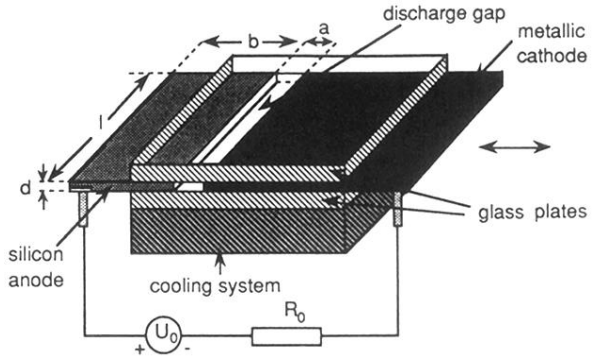

FIG. 1. Experimental setup of the gas-discharge device.

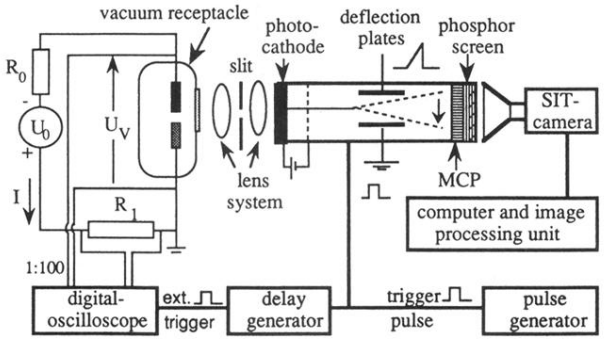

FIG. 2. Setup for measuring the spatiotemporal behavior of the current-density distribution in the discharge gap.

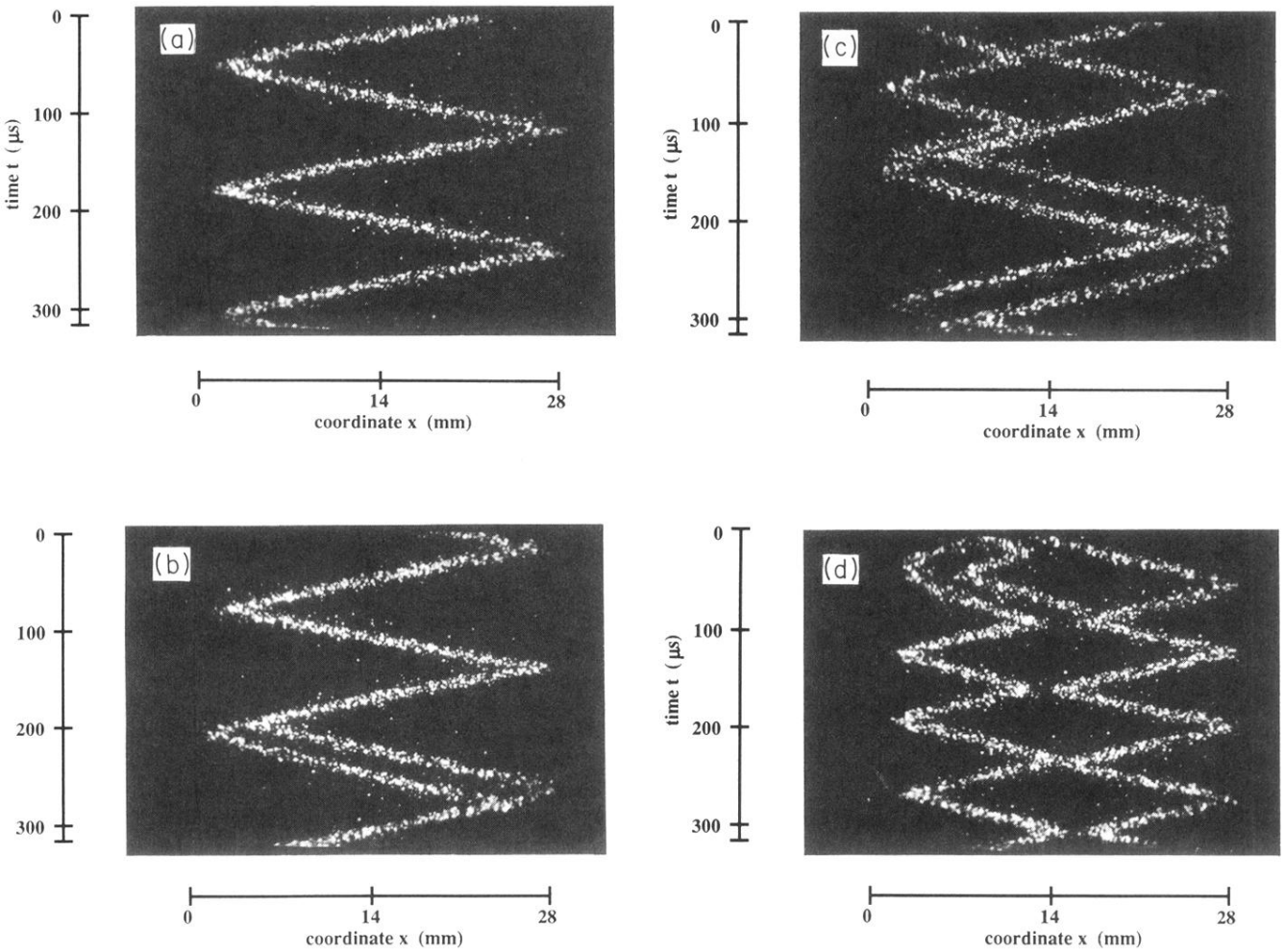

FIG. 7. Streak-camera photographs of rocking filament scenarios for the case of a high-resistivity electrode and for increasing averaged total current I_a. Due to the increase of the number of solitary filaments and due to their interactions turbulence appears. The parameters are $l=28$ mm, $b=8$ mm, $d=0.25$ mm, $\rho=2.6$ kΩ cm, $p=20$ hPa, $a=3.25$ mm, and $R_0=250$ kΩ. (a) $U_0=500$ V, $I_a=0.59$ mA; (b) $U_0=518$ V, $I_a=0.65$ mA; (c) $U_0=573$ V, $I_a=0.89$ mA; (d) $U_0=585$ V, $I_a=0.94$ mA; (e) $U_0=670$ V, $I_a=1.23$ mA; (f) $U_0=723$ V, $I_a=1.43$ mA; (g) $U_0=766$ V, $I_a=1.60$ mA; (h) $U_0=847$ V, $I_a=1.88$ mA.

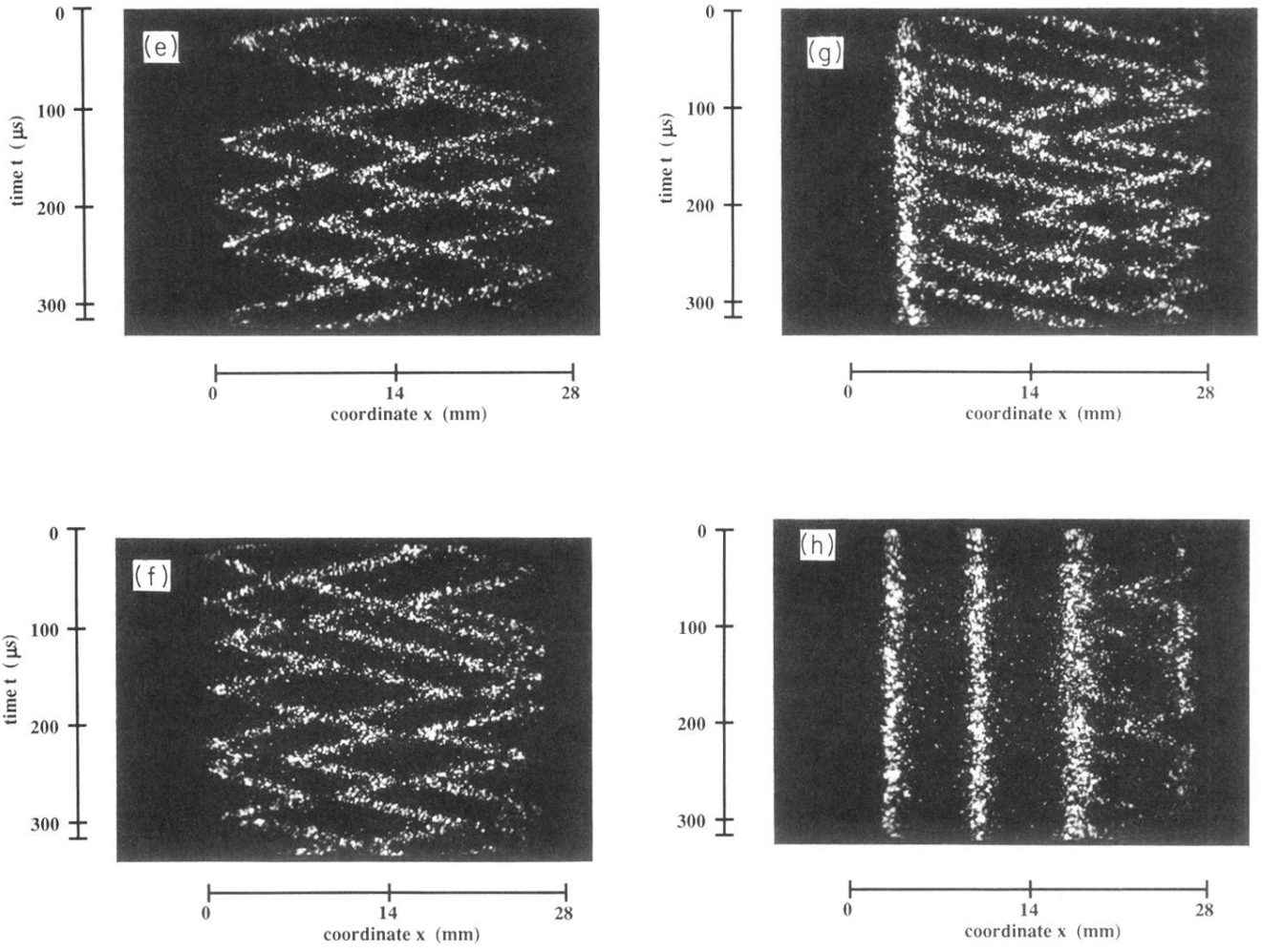

FIG. 7. (*Continued*).

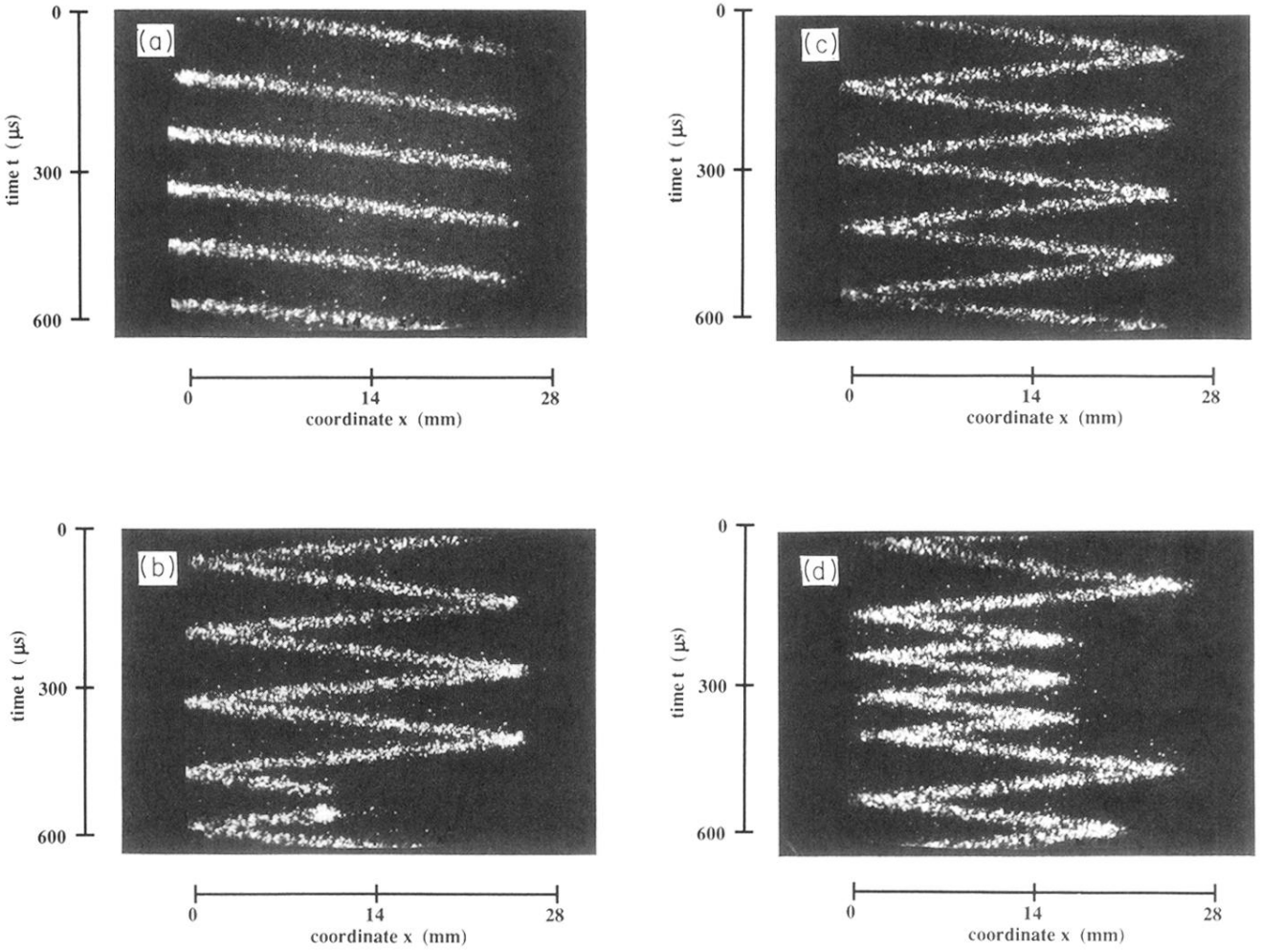

FIG. 8. Streak-camera photographs of the generation of rocking filaments for the low-resistivity semiconductor electrode system for increasing voltage U_0 corresponding to increasing average total current I_a. Due to the interaction of the filaments a turbulent behavior in the form of spatiotemporal intermittency appears. The parameters are $l=28$ mm, $b=10$ mm, $d=0.28$ mm, $\rho=0.9$ kΩ cm, $p=14$ hPa, $a=4.8$ mm, and $R_0=1$ MΩ. (a) $U_0=800$ V, $I_a=0.4$ mA; (b) $U_0=880$ V, $I_a=0.5$ mA; (c) $U_0=950$ V, $I_a=0.6$ mA; (d) $U_0=1090$ V, $I_a=0.74$ mA; (e) $U_0=1125$ V, $I_a=0.78$ mA; (f) $U_0=1340$ V, $I_a=1.0$ mA; (g) $U_0=1830$ V, $I_a=1.5$ mA; (h) $U_0=2010$ V, $I_a=1.7$ mA.

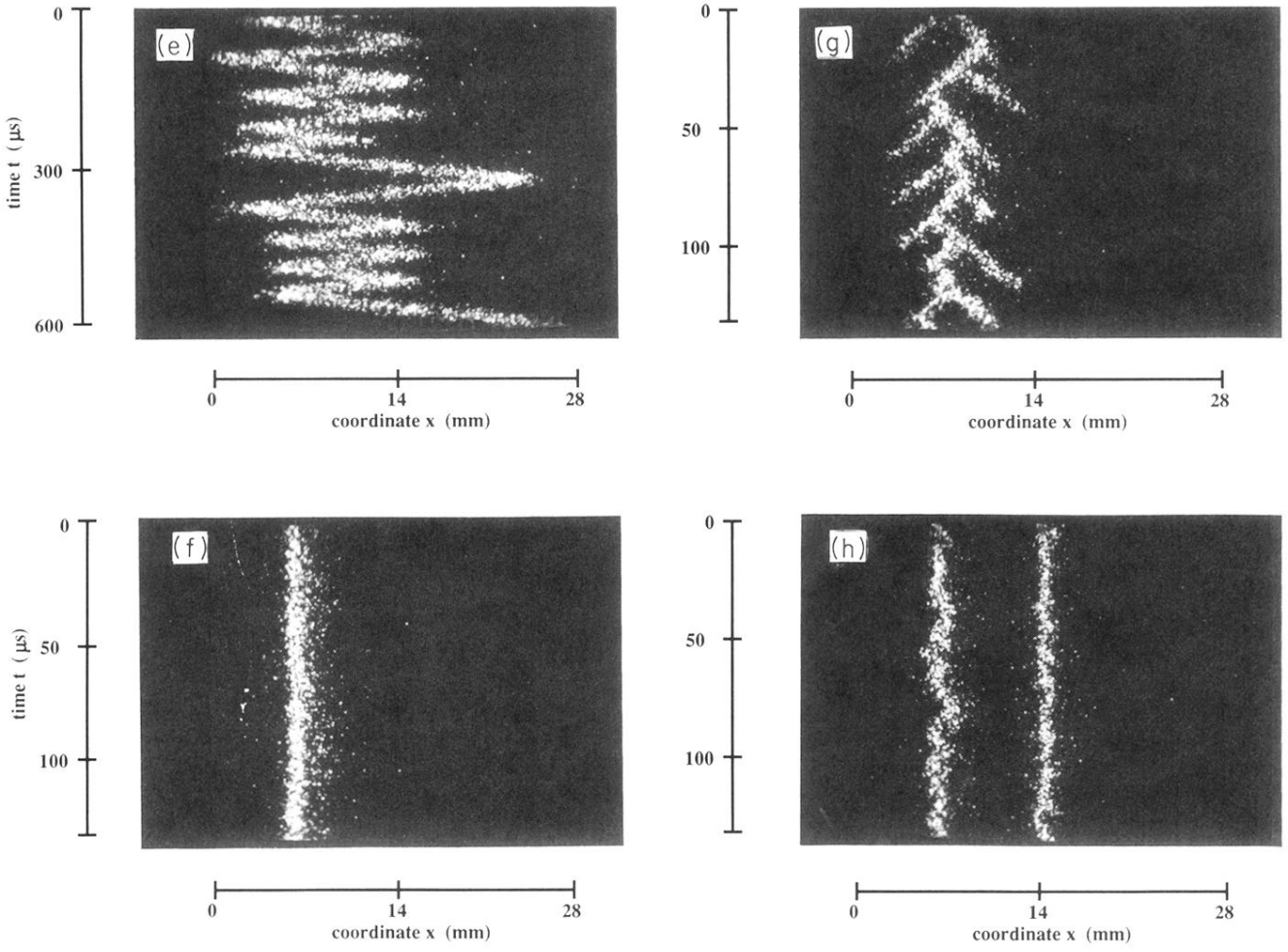

FIG. 8. (*Continued*).